The sensitivity of ECG contamination to surgical implantation site in adaptive closed-loop neurostimulation systems

Wolf-Julian Neumann[1], Majid Memarian Sorkhabi[2], Moaad Benjaber[2], Lucia K. Feldmann[1], Assel Saryyeva[3], Joachim K. Krauss[3], Maria Fiorella Contarino[4], Tomas Sieger[5], Robert Jech[5], Gerd Tinkhauser[6], Claudio Pollo[7], Chiara Palmisano[8], Ioannis U. Isaias[8], Daniel Cummins[9], Simon J. Little[9], Philip A. Starr[10], Vasileios Kokkinos[11], Schneider Gerd-Helge[12], Todd Herrington[13], Peter Brown[2], R. Mark Richardson[10], Andrea A. Kühn[1], Timothy Denison[2]

Corresponding author: Timothy Denison

Affiliations:

[1]Movement Disorder and Neuromodulation Unit, Department of Neurology, Charité - Universitätsmedizin Berlin, Chariteplatz 1, 10117, Berlin, Germany
[2]MRC Brain Network Dynamics Unit, Nuffield Department of Clinical Neurosciences, University of Oxford, United Kingdom
[3]Department of Neurosurgery, Medizinische Hochschule Hannover, Hannover, Germany
[4]Department of Neurology, Leiden University Medical Center, Leiden & Haga Teaching Hospital, The Hague, The Netherlands
[5]Department of Neurology, Charles University, 1st Faculty of Medicine and General University Hospital, Prague, Czech Republic
[6]Department of Neurology, Bern University Hospital and University of Bern, Bern, Switzerland
[7]Department of Neurosurgery, Bern University Hospital and University of Bern, Bern, Switzerland
[8]Department of Neurology, University Hospital of Würzburg and Julius Maximilian University of Würzburg, Würzburg, Germany
[9]Department of Neurology, University of California, San Francisco, San Francisco, CA 94143, USA
[10]Department of Neurological Surgery, University of California, San Francisco, San Francisco, CA 94143, USA
[11]Department of Neurosurgery, Massachusetts General Hospital and Harvard Medical School, Boston, MA, USA.
[12]Department of Neurosurgery, Charité - Universitätsmedizin Berlin, Chariteplatz 1, 10117, Berlin, Germany
[13]Department of Neurology, Massachusetts General Hospital and Harvard Medical School, Boston, MA, USA.

Authorship contributions:

WJN and TD conceptualized the study, performed statistical analysis, and drafted the manuscript. MMS, MB, PB and TD conceptualized and performed the modelling analysis. LKF, AS, JKK, MFC, TS, RJ, GT, CP, IUI, SL, PS, VK, GH, TH, RMR and AAK acquired and analysed electrophysiological data. AAK and TD provided funding for the study. All authors revised and approved the final version of the manuscript.

Abstract (structured, 200 words):

Objective: Investigate neural signal contamination with electrocardiographic (ECG) activity in bidirectional implantable neurostimulation systems for closed-loop stimulation in neurological diseases.

Methods: Electric field modelling was used to predict the relevance of implant location to ECG contamination in neural signals recorded with implantable devices. Signals from 335 recording streams in 136 hemispheres from 85 patients were visually inspected for ECG contamination to validate the model. Implant sites were categorized into left, right subclavicular hemibody and cranial implant.

Results: Our model predicted significant dependence of the ECG amplitude on implant location, ranging from a 4x difference with chest location to a 1000x suppression with cranial implants. The impact on neural recordings depends on the difference between ECG signal and noise floor of the recording. Empirically, we demonstrate that severe ECG contamination was more than 3.2x higher in left implants (48.3%), when compared to right implants (15.3%). Cranial implants did not show ECG contamination.

Conclusion: Given the relative frequency of corrupted neural signals, we conclude that implant location will have significant impact on patient recruitment and feasibility in multicenter clinical trials for adaptive brain stimulation. Prospectively, the impact of implant location on signal fidelity should be carefully considered in the surgical planning process.

Main (no more than 1758/1500 words):

Introduction:

Invasive neurostimulation can modulate neural activity and alleviate symptoms in a variety of severe neurological and psychiatric disorders. [1,2] Current advances in deep brain stimulation (DBS) research investigate the utility of closed-loop adaptive DBS based on neural feedback signals recorded directly from the stimulation electrodes. [3,4] Most prominently, subthalamic beta activity (13 - 35 Hz) in Parkinson's disease was shown to reflect parkinsonian motor sign severity that rapidly follows the clinical response to treatment and is a promising candidate for adaptive deep brain stimulation (aDBS). [5,6] Similarly, in patients with epilepsy, seizure activity can inform rapid therapeutic intervention. [7] In such scenarios, clinical success of demand-dependent treatment adaptation depends on the reliability of the feedback signal. Neurophysiological recordings are notoriously prone to electrical artifacts. The strongest source of electrical activity in the human body is the heart, and the frequency content of cardiac activity overlaps many brain signals of interest (Figure 1). Since the first experience with sensing enabled implantable DBS devices, ECG contamination remains an unresolved problem rendering a significant number of recordings unusable. In the present study, we investigate the relationship between the electric field of cardiac activity, implant location, and contamination of neural signals recorded.

Methods:

Modelling

Physiological modeling can be used to investigate the effect of the reference electrode placement on the induced cardiac artifacts. [8] Here, the heart is treated as a single current dipole source in the thorax modelled to have a uniform electrical conductivity. [8] In our computational model using COMSOL software, the current- source dipole heart model is surrounded by a homogeneous volume conductor (average tissue conductivity = 0.33 S/m) with the shape of a three-dimensional human torso, consisting of 2 mm^3 elements (Figure 1A). The magnitude of the electric current dipole moment is assumed

to be 1 (mA meter). This model was solved linearly through finite element methods. To predict the maximum possible artifact value, the hypothetical locations of the dipole points are examined in different scenarios around the heart locus. The net voltage induced across the lead was then calculated by integrating the electric field between device location and leads placed in the center of the cranium.

Empirical data

The study was carried out in accordance with the Declaration of Helsinki and was approved by the internal review board of Charité – Universitätsmedizin Berlin. To validate the predictions of our model, we visually inspected recordings for ECG contamination. Therefore, archival local field potential (LFP) recordings from 8 international neuromodulation centers in 86 implants in 85 patients were inspected for evidence of ECG. From this cohort, 53 patients have undergone implantation of Medtronic Percept DBS pulse generators (21 left subclavicular, 1 left abdomen, 29 right subclavicular, 1 right abdomen, 1 both left and right subclavicular; see Table 1). Most commonly DBS was applied biltaterally (one lead in each hemisphere), 4 implants only had leads in one hemisphere connected (unilateral). Calibration Tests were performed bipolarly for contact pairs 0-2 and 1-3, with 0 being the lowermost contact. This resulted in 2 channels per lead. One channel from one patient had to be excluded due to impedance issues, resulting in 207 channels overall. Additionally, 32 patients have been implanted with a neurostimulation system mounted to the skull (cranial mount) for treatment refractory epilepsy therapy (RNS Neuropace). For Percept data, bipolar calibration test recordings of ~20 s length were visualized using our open-source Perceive Toolbox (www.github.com/neuromodulation/perceive/) in Matlab (The Mathworks). For cranial mounts, visual inspection was performed from routine recordings. ECG artifacts were identified based on the presence of characteristic sharp QRS-like signal deflections of ~150-200 ms width with stereotypic amplitudes occurring at 60-100 bpm. Artifacts were categorized into absent, minor, and severe (see Figure 1B), as some recordings had visible but low amplitude contamination, e.g. with just the tip of the QRS complex close to the level of neural activity. Statistical comparison of implant location and observed ECG

contamination were performed by aggregating channel counts per implant and using the exact version of non-parametric Wilcoxon's rank sum tests.

Results:

Electric field models predict peak ECG contamination in left chest

The potential difference values of cardiac activity were simulated to predict ECG artifact contamination. The induced voltage at the measurement leads is estimated by integrating the electric fields, approximated using FEM to be 5.02 A/m2 and 15.2 V/m for subclavicular (Figure 1A) and 42.7 μA/m2 and 94 μV/m for cranial implant regions. Cardiac artifacts are estimated to be on the order of 1-3 mV for a chest mounted device and between 4.1 and 6.5 times greater for the left compared to right side, depending on the specific location of the current dipole. The cranial mounted system results in an estimated signal of approximately 100 uV and is less susceptible to placement.

The final voltage that is seen in the signal chain depends on the actual common mode rejection ratio (CMRR) typically ranging -60-to-40dB. Based on this, artifact amplitude can be predicted to exceed the LFP (~1-20 μVrms) in chest-mounted devices. In cranial mount devices the artifact will be below the amplifier noise floor and undetectable.

Empirical artifact frequency

Visual inspection of LFP recorded in subclavicular implants (N=54 Medtronic Percept) revealed higher proportion of overall ECG contaminated signals (Figure 1C) in left (58/89 channels, 65.2%, N=23 devices) vs. right implants (41/118 channels, 34.8%, N=31 devices, p=0.006). Importantly, severe ECG contamination rendering the signals unusable for therapeutic algorithms, were three times more likely to occur in left (43/89, 48.3%, N=23) vs. right implant locations (18/118, 15.3%, N=31, p=0.001). Given that each patient has 2 potential recording channels per lead, the availability of at least one usable signal stream per lead and hemisphere is particularly relevant for recruitment and planning of clinical aDBS trials. For bilateral use, at least one unaffected channel per hemisphere and lead is required (Figure 1D). This was the case in only 45.5% (10/22) of patients with left, compared to 89.3% (25/28, p=0.002) patients with right implants and

two connected leads (unilateral implants excluded). If unilateral recordings were to prove sufficient for bilateral control of the stimulator in aDBS this would have been possible in 63.6% of left implants (14/22) and 96.4% of right implants (27/28, p=0.008).

ECG was absent in neural data from cranial implants (32 patients, 128 channels), yielding a significant difference to both left and right subclavicular implants (all p<0.01).

Discussion

The present study demonstrates that ECG contamination of neural signals recorded with novel implantable devices attenuates with relation to the electric field of the heart. We derive two major consequences from this. First, for subclavicular systems, the device is highly susceptible to its location relative to the cardiac dipole. In practice, patients with left implants are more likely to exhibit ECG in neural recordings than patients with right implants. From our empirical data, only 45% of patients with left hemibody implants were fit for bilateral adaptive stimulation, compared to 89% in patients with right implants. The second implication is that even right subclavicular implants can suffer from ECG contamination, especially in low amplitude subcortical signals that are being explored for DBS therapies. Beyond aDBS for Parkinson's disease, electrophysiological biomarkers have been described in dystonia [9], Tourette's syndrome [10] and other neuropsychiatric disorders. Further technical improvements for artifact suppression is needed to offer new therapeutic advances to all DBS patients.

Origin of Susceptibility to Artifacts in Brain Sensing Interfaces

Local field potentials are measured as a differential signal from the leads implanted in the brain. The LFP signal can range from 1-20 μVrms [11], and the majority of LFP oscillations are in low frequency bands, ranging from 1 Hz to 100 Hz, where artifacts are also present. When a DBS device is implanted, the device case can act, sometimes inadvertently, as the system's reference. In theory, the ECG artifact can couple into the sensing input chain as a common mode signal. In an implantable system, the common mode rejection ratio can be undermined by input impedance mismatch. Such mismatch can occur between the tissue-electrode interface and the front-end amplifier, through impedance differences

along the lead and extension interfaces and among some more specific filter and capacitor components used as hardware building blocks in DBS systems.

Mitigation of ECG contamination in neural recordings from implantable devices

Our study suggests that strategic placement distant to the cardiac electric dipole can mitigate ECG contamination. We should note there are alternative approaches to address artifact susceptibility. These methods include improving the matching of the signal chain by improving the electrical properties of leads and extensions, lowering the tissue-electrode interface impedance with new coatings, or exploring alternative signals at frequencies outside of the artifact susceptibility. One or more of these might be adopted in future systems. Moreover, given the proximity of the ECG artifact to the LFP noise floor, higher amplitude signals, e.g. recorded with electrocorticography, will not suffer from ECG and may be viable for certain aDBS applications [6,12–14]. Finally, given the brevity of the high amplitude QRS component, post-hoc processing can restore a significant portion (~80%) underlying neural activity in many contaminated signals, but even if this proves possible in real-time it will involve additional power consumption.

Limitations

The evaluation of ECG artefact was visual. In the future we hope to validate our findings with objective measurements of ECG contamination. Importantly, even though we demonstrate data from a representative sample size, we only included data recorded from a single device for subclavicular (Medtronic Percept) and cranial (RNS Neuropace) implants. However, a previous generation of subclavicular devices (Medtronic PC+S) had corrupted recording streams often excluded them from otherwise valuable studies. [15] For cranial implants, higher amplitude signals from cortical recording locations were likely additionally beneficial and may represent a bias in the ECG contamination statistic. For this reason we also directly contrast left and right subclavicular implants.

It is worth noting that although our focus was on ECG artifacts, susceptibility to motion artifacts will follow a similar pattern that will require further attention. The data from cranial mount systems would suggest that the minimal physical motion of the lead and device

will help mitigate these issues as well, but the root cause of these issues remains under investigation.

In conclusion, sensing enabled IPGs for neurostimulation can suffer from ECG contamination that is stronger and more frequent in left subclavicular implant locations, when compared to right or cranial implants. Mitigation strategies include adjustment of implant location, alternative higher amplitude signal sources and post-hoc processing. Given the absence of ECG in cranial implants, our data suggest that future bidirectional brain computer interfaces should explore the utility of cranial mounts to avoid ECG contamination altogether.

Acknowledgements:
The authors would like to thank Dr. R. Zutt (Dept. of Neurology Hagaziekenhuis), Dr. N.A. van der Gaag, and Dr. C.F Hoffmann (Dept of Neurosurgery, Hagaziekenhuis) for the clinical care of the patients and help with data acquisition. This study was funded by the Deutsche Forschungsgemeinschaft (DFG, German Research Foundation) – Project-ID 424778381 – TRR 295 to WJN, IUI and AAK, the Medical Research Council, United Kingdom (MC_UU_12024/1) to PB, the Czech Ministry of Education under grant AZV: NV19-04-00233 and by Charles University under research project Progres Q27 to RJ.

Disclosures:

Dr. Neumann has nothing to disclose. Dr. Majid Memarian Sorkhabi has nothing to disclose. Mr. Benjaber has nothing to disclose. Dr. Feldmann has nothing to disclose. Dr. Saryyeva has nothing to disclose. Dr. Krauss reports personal fees from Medtronic, personal fees from Boston Scientific, outside of the submitted work. Dr. Contarino reports non-financial support from Boston Scientific, grants and other from Medtronic, other from CHDR, grants from AbbVie, non-financial support from Global Kinetics Corporation, outside the submitted work. Dr. Tinkhauser has nothing to disclose. Dr. Pollo received consultancy fees from Boston and Abbott and is Co-founder of Aleva Neurotherapeutics, outside of the submitted work. Dr. Sieger has nothing to disclose. Dr. Jech reports honoraria and consultancies from Ipsen, Desitin and Cardion, outside the submitted work. Dr. Palmisano has nothing to disclose. Dr. Isaias reports honoraria from Medtronic Inc and grants from Newronika Srl, outside the submitted work. Dr. Cummins has nothing to disclose. Dr. Little has nothing to disclose. Dr. Starr reports research support, in the form of investigational devices provided at no charge, from Medtronic Inc., outside the submitted work. Dr Kokkinos has nothing to disclose. Dr. Schneider reports Speakers honoraria from Medtronic, Abbot and Boston Scientific, outside of the submitted work. Dr. Herrington discloses personal fees from Medtronic and Boston Scientific, outside the submitted work. Dr. Brown reports grants and personal fees from Medtronic, outside the submitted work. Dr. Richardson has nothing to disclose. Dr. Kühn is in the advisory board of Medtronic and Boston Scientific and reports personal fees from Medtronic and Boston Scientific, outside the submitted work. Dr. Denison reports personal fees from Medtronic, during the conduct of the study; other from Bioinduction (cranial mount system), outside the submitted work.

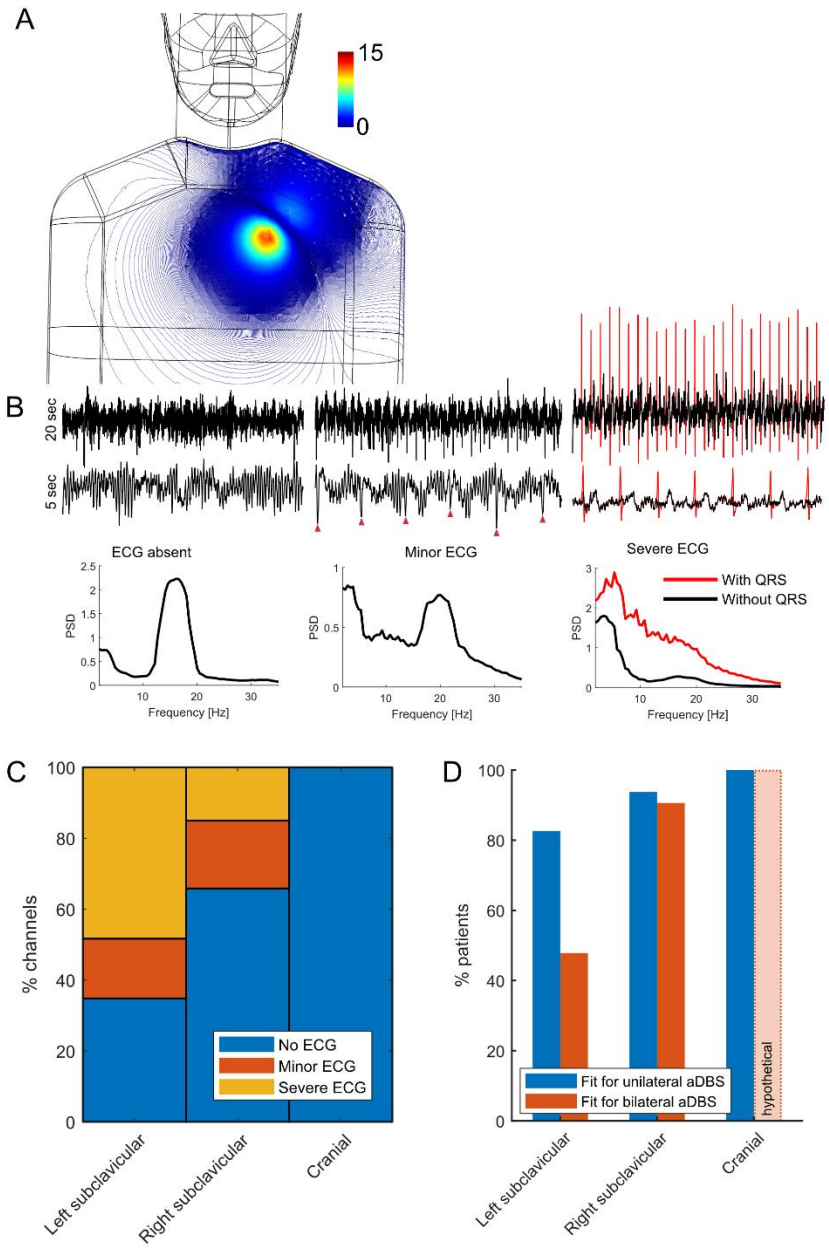

Figure 1: ECG artifacts contaminate neural signals in subclavicular implants. Modelling the electric field (A) throughout the cardiac cycle suggests a higher susceptibility for ECG artifacts in the left, when compared to right chest. Exemplar subthalamic LFP and resulting power spectral densities (B) recorded from patients with Parkinson's disease in Berlin demonstrate the artifact categories (absent, minor, severe from left to right). For offline processing, the QRS complex can be identified (e.g. red arrow in minor contamination) and removed (red line in severe contamination category, see https://github.com/neuromodulation/perceive). In the severe contamination example replacing 4.37 s affected by QRS (red high amplitude discharges) with mirrored padding could restore an underlying beta oscillatory peak (black PSD), demonstrating the severity of beta frequency contamination from the QRS complex alone (red PSD). ECG contaminated channels were present in left and right subclavicular implants (C), rendering a significant portion of DBS leads unusable for aDBS trials (D).

Left subclavicular implants					Right subclavicular implants				
N	**DIS**	**TGT**	**BAD CH**	**BAD HEM**	**N**	**DIS**	**TGT**	**BAD CH**	**BAD HEM**
1~	DYT	GPi	3	2	1	PD	STN	2	0
2	DYT	GPi	2	1	2	PD	STN	0	0
3	PD	STN	1	0	3	PD	STN	0	0
4	PD	STN	0	0	4	PD	GPi	0	0
5	PD	STN	1	0	5	PD	STN	0	0
6	PD	STN	1	0	6	PD	GPi	0	0
7	PD	STN	4	2	7	PD	GPi	0	0
8	PD	STN	3	1	8	PD	GPi	1	0
9	PD	STN	0	0	9	PD	STN	0	0
10	PD	STN	4	2	10	PD	STN	1	0
11	PD	GPi	3	1	11	DYT	GPi	0	0
12	PD	STN	0	0	12	PD	STN	0	0
13	PD	STN	0	0	13	PD	STN	0	0
14#	DYT	GPi	4	2	14	PD	STN	0	0
15	PD	STN	4	2	15	PD	GPi	0	0
16	PD	STN	0	0	16	OCD	AIC	1	0
17*	PD	GPi	0	0	17	PD	GPi	4	2
18§	TIN	CAUD	2	1	18	PD	GPi	0	0
19	PD	STN	2	0	19	ET	VIM	0	0
20	ET	VIM	3	1	20	PD	GPi	0	0
21	PD	STN	0	0	21*#~	DYT	GPi	0	0
22	PD	STN	3	1	22*	DYT	GPi	0	0
23	PD	STN	3	1	23*	PD	GPi	1	0
					24	PD	GPi	1	0
					25	PD	STN	2	1
					26	DYT	GPi	0	0
					27	DYT	GPi	4	2
					28	PD	STN	1	0
					29	DYT	GPi	0	0
					30	PD	STN	0	0
					31	ET	VIM	0	0

Table 1: Subclavicular implant details. Abbreviations: AIC = anterior limb of internal capsule; BAD CH = Number of channels with severe ECG contamination; BAD HEM = Number of hemispheres with all channels with severe ECG contamination; CAUD = Caudate nucleus; DIS = Disease; DYT = Dystonia, ET = Essential Tremor; GPi = internal pallidum; OCD = obsessive compulsive disorder; PD = Parkinson's disease; STN = subthalamic nucleus; TGT = Target; TIN = Tinnitus; VIM = ventral intermediate nucleus of thalamus; §one channel excluded; *unilateral implants; #depict two separate percept implants in a single patient; ~abdominal implants.

References:

1 Cagnan H, Denison T, McIntyre C, *et al.* Emerging technologies for improved deep brain stimulation. *Nat Biotechnol* 2019;**37**:1024–33. doi:10.1038/s41587-019-0244-6

2 Krauss JK, Lipsman N, Aziz T, *et al.* Technology of deep brain stimulation: current status and future directions. Nat. Rev. Neurol. 2020. doi:10.1038/s41582-020-00426-z

3 Little S, Pogosyan A, Neal S, *et al.* Adaptive deep brain stimulation in advanced Parkinson disease. *Ann Neurol* Published Online First: 2013. doi:10.1002/ana.23951

4 Arlotti M, Marceglia S, Foffani G, *et al.* Eight-hours adaptive deep brain stimulation in patients with Parkinson disease. *Neurology* Published Online First: 2018. doi:10.1212/WNL.0000000000005121

5 Kühn AA, Kempf F, Brücke C, *et al.* High-frequency stimulation of the subthalamic nucleus suppresses oscillatory beta activity in patients with Parkinson's disease in parallel with improvement in motor performance. *J Neurosci* 2008;**28**:6165–73. doi:28/24/6165 [pii] 10.1523/JNEUROSCI.0282-08.2008

6 Neumann W-J, Turner RS, Blankertz B, *et al.* Toward Electrophysiology-Based Intelligent Adaptive Deep Brain Stimulation for Movement Disorders. *Neurotherapeutics* 2019;**16**. doi:10.1007/s13311-018-00705-0

7 Kokkinos V, Sisterson ND, Wozny TA, *et al.* Association of Closed-Loop Brain Stimulation Neurophysiological Features with Seizure Control among Patients with Focal Epilepsy. *JAMA Neurol* 2019;**76**:800–8. doi:10.1001/jamaneurol.2019.0658

8 Sorkhabi MM, Benjaber M, Brown P, *et al.* Physiological Artifacts and the Implications for Brain-Machine-Interface Design. In: *2020 IEEE International Conference on Systems, Man, and Cybernetics (SMC)*. IEEE 2020. 1498–1498. doi:10.1109/SMC42975.2020.9283328

9 Neumann W-J, Horn A, Ewert S, *et al.* A localized pallidal physiomarker in cervical dystonia. *Ann Neurol* 2017;**82**:912–24. doi:10.1002/ana.25095

10 Neumann W-J, Huebl J, Brücke C, *et al.* Pallidal and thalamic neural oscillatory patterns in Tourette syndrome. *Ann Neurol* Published Online First: 15 August 2018. doi:10.1002/ana.25311

11 Stanslaski S, Afshar P, Cong P, *et al.* Design and validation of a fully implantable, chronic, closed-loop neuromodulation device with concurrent sensing and stimulation. *IEEE Trans Neural Syst Rehabil Eng* 2012;**20**:410–21. doi:10.1109/TNSRE.2012.2183617

12 Swann NC, De Hemptinne C, Thompson MC, *et al.* Adaptive deep brain stimulation for Parkinson's disease using motor cortex sensing. *J Neural Eng* Published Online First: 2018. doi:10.1088/1741-2552/aabc9b

13 Opri E, Cernera S, Molina R, *et al.* Chronic embedded cortico-thalamic closed-loop deep brain stimulation for the treatment of essential tremor. *Sci Transl Med* 2020;**12**:eaay7680. doi:10.1126/scitranslmed.aay7680

14 Gilron R, Little S, Perrone R, *et al.* Chronic wireless streaming of invasive neural recordings at home for circuit discovery and adaptive stimulation. *bioRxiv* 2020;:2020.02.13.948349. doi:10.1101/2020.02.13.948349

15 Anidi C, O'Day JJ, Anderson RW, *et al.* Neuromodulation targets pathological not physiological beta bursts during gait in Parkinson's disease. *Neurobiol Dis* 2018;**120**:107–17. doi:10.1016/j.nbd.2018.09.004